Temporal dynamics analysis reveals that concurrent working memory load eliminates the Stroop effect through disrupting stimulus-response mapping

Yafen Li[a], Yixuan Lin[b], Qing Li[c], Yongqiang Chen[c], Zhifang Li[b], Antao Chen[a,*]

[a] School of Psychology, Shanghai University of Sport, Shanghai 200438, China

[b] School of Psychology and Cognitive Science, East China Normal University, Shanghai 200062, China

[c] Faculty of Psychology, Southwest University, Chongqing 400715, China

*Corresponding author:

School of Psychology, Shanghai University of Sport, Yangpu District, Shanghai 200438, China.

Email: chenantao@sus.edu.cn

Abstract

Concurrent verbal working memory task can eliminate the color-word Stroop effect. Previous research, based on specific and limited resources, suggested that the disappearance of the conflict effect was due to the memory information preempting the resources for distractors. However, it remains unclear which particular stage of Stroop conflict processing is influenced by working memory loads. In this study, electroencephalography (EEG) recordings with event-related potential (ERP) analyses, time-frequency analyses, multivariate pattern analyses (MVPA), and representational similarity analyses (RSA) were applied to provide an in-depth investigation of the aforementioned issue. Subjects were required to complete the single task (the classical manual color-word Stroop task) and the dual task (the Sternberg working memory task combined with the Stroop task), respectively. Behaviorally, the results indicated that the Stroop effect was eliminated in the dual-task condition. The EEG results showed that the concurrent working memory task did not modulate the P1 and alpha bands. However, it modulated the sustained potential (SP), late theta (740-820 ms), and beta (920-1040 ms) power, showing no difference between congruent and incongruent trials in the dual-task condition but significant difference in the single-task condition. Importantly, the RSA results revealed that the neural activation pattern of the late theta was similar to the response interaction pattern. Together, these findings implied that concurrent working memory task eliminated the Stroop effect through disrupting stimulus-response mapping.

Keywords: Stroop effect; working memory; electroencephalography; multivariate pattern analysis

1. Introduction

It is critical to effectively deal with the conflict between task-relevant and task-irrelevant information to successfully complete goal-directed behaviors. One of the most commonly employed experimental paradigms for evaluating conflict processing is the color-word Stroop task, which is characterized by lower accuracy and/or longer reaction times (RT) in incongruent trials compared to congruent trials (Stroop, 1935). Of note, an interesting phenomenon is that concurrent verbal working memory task can reduce or even eliminate the Stroop conflict (Kim et al., 2005; Luna et al., 2020; Park et al., 2007; Zhao et al., 2014). In terms of the load theory based on multiple resources, cognitive resources are limited while specific to different cognitive processes. When substantial resources are allocated to maintaining memory information, the resources required to process same-dimension distractors are occupied, reducing the interference caused by the distractors (Brockhoff et al., 2022; Luna et al., 2020; Park et al., 2007). Although this theory attempts to explain the disappearance of the Stroop conflict, its description remains relatively vague, and it does not further reveal which specific processes are influenced during Stroop processing.

Stroop conflict processing should be understood not as a single process but as multiple successive subprocesses, including stimulus processing, stimulus-response mapping, and response output stage (Banich, 2019; Parris et al., 2022; Viviani et al., 2023). Related research suggests that there might be two possibilities. The first one is that concurrent working memory task primarily decreases the neural encoding of

perceptual visual features, known as the early-stage modulation hypothesis. The sensory recruitment hypothesis posits that the sensory cortex is crucial for maintaining visual content by modulating sensory gain, thereby biasing processing towards relevant stimuli (Hallenbeck et al., 2021; Wolff et al., 2020). Moreover, several researchers have suggested that the Stroop effect relies more on the input-driven allocation of attention to perceptual features (Algom et al., 2022; Bugg & Crump, 2012; Haciahmet et al., 2023; Schmidt, 2019). Accordingly, these views suggest that working memory maintenance competes for neural resources with the lower-level visual encoding of distractors, hindering conflict formation at an early stage. Besides, the second one is that concurrent working memory task primarily weaken higher-level processing, termed the late-stage modulation hypothesis. The theoretical underpinning is that the working memory system comprises not only sensory buffers but also a central system (Baddeley, 2012) that mainly recruits the prefrontal cortex, partially overlapping with the brain networks involved in Stroop conflict processing (Friehs et al., 2020; Okayasu et al., 2023). Furthermore, some research indicated that filtering out highly familiar and easily processed semantic information during the early sensory processing stage is difficult for individuals (Augustinova et al., 2019; Cavanagh & Frank, 2014; Itthipuripat et al., 2019). Consistent with this hypothesis, both relevant and irrelevant sensory inputs receive comprehensive semantic processing, while working memory load constrains the process of binding higher-level semantic codes with responses, potentially influencing the subsequent response output stage. Overall, the two hypotheses, although distinct,

are not mutually exclusive and can be inspected from a time-dynamic perspective.

In the present study, a single task (the classical manual Stroop task) and a dual task (the Sternberg working memory task combined with the Stroop task) were employed to explore the aforementioned hypotheses with electroencephalography recording of high temporal resolution. Several event-related potentials (ERP) highly relevant to Stroop conflict processing will be focused on in this study. Previous studies have proposed that within cognitive control mechanisms, P1 signifies the earliest stage of top-down processes in early sensory processing, gating the direction of information processing in the brain (Klimesch et al., 2007). Moreover, the incongruent trials in the Stroop task evoke smaller positive P1 than congruent trials, supporting that P1 is a valid index in conflict processing (Yu et al., 2015). Additionally, numerous studies have identified two ERP components exclusively elicited by the Stroop task (i.e., the N450 and the sustained potential (SP)). N450 is a frontal-central negative deflection that exhibits greater negativity in incongruent trials compared to congruent trials within 350-500 ms after stimulus onsets, which is typically interpreted as conflict monitoring, the process of evaluating conflict levels and communicating the conflict information to control systems (Coderre et al., 2011; Heidlmayr et al., 2020; Xu et al., 2024). As for the SP component, it shows a centro-parietal positive deflection from approximately 600 ms to 1000 ms in incongruent conditions, which is regarded as an index of conflict resolution (Di Russo & Bianco, 2023; Donohue et al., 2016; Heidlmayr et al., 2020; Vo et al., 2021). In all, these ERP components, which are distinctly time-sequential, can help explore the dynamic

effects of working memory on Stroop conflict processing.

In addition to the ERP components, conflict processing also involves various neural oscillatory activities. First, extensive research has found that mid-frontal theta (4-7 Hz) power increases in conflict situations with the time windows of early and late theta band effects in stimulus-locked analyses corresponding to those of the N450 and SP effects, which suggests that early and later theta power reflects conflict detection and resolution processes, respectively (Brilliant et al., 2024; Haciahmet et al., 2023; Senoussi et al., 2022; Xu et al., 2024; Zhao et al., 2015). Second, alpha oscillations (8-13 Hz) can serve as a neural inverse index of mental activity or alertness, while a decrease in alpha power reflects increased alertness or enhanced attentional inhibition of distractors (Arakaki et al., 2022; Tafuro et al., 2019; Zhou et al., 2023; Zhu et al., 2023). Third, previous study has shown that the response incongruent trial evokes a small beta power than the stimulus incongruent trial in the Stroop task (Zhao et al., 2015). The suppressed effect of the beta power most likely reflects the inhibition of proponent responses, associated with motion preparation (Böttcher et al., 2023; Chung et al., 2024; Wendiggensen et al., 2022; Zhao et al., 2015). Accordingly, these frequency bands can provide a comprehensive characterization of the Stroop conflict processing.

It is worth realizing that neural oscillations are not characterized by a pre-determined time window like ERPs. However, multivariate pattern analysis (MVPA) can help to solve the difficulty of hypothesizing which frequency band or the time window is changed in the Stroop task. As a data-driven technique, MVPA provides

novel insight into the differences between two conditions by identifying the features that contribute most to classification (Li et al., 2023; Lin et al., 2023; Meier et al., 2012). Therefore, the present study will combine time-frequency analysis and MVPA to inspect the dynamic neural characteristics of the modulation of working memory on Stroop conflict processing at the neural oscillatory level.

Notably, even if differences are found in ERPs or neural oscillations, the extent to which they are linked to behavior is an interesting question. Representational similarity analysis (RSA) is applied to build a connection between behavior and neural activities in the present study (Kriegeskorte & Kievit, 2013). Recent studies have suggested that RSA is a reliable way to uncover the neural mechanisms behind conflict processing (Freund et al., 2021; Yang et al., 2023), which helps identify which neural activities are central to the influence of working memory on Stroop conflict processing. Overall, the present study employs EEG technology, through MVPA and RSA, in an attempt to comprehensively uncover the dynamic neural underlying the elimination of the Stroop effect influenced by working memory when the dimensions of memory information and distractors overlap.

2. Results

2.1. Behavioral results

For behavioral analysis, a two-way repeated measures ANOVA (task type: single task vs. dual task × congruency: congruent vs. incongruent) was performed on RTs. The results showed that the RTs of the single-task condition were faster than dual-task

condition (main effect of task type: $F_{(1, 31)} = 113.28$, $p < 0.001$, $\eta_p^2 = 0.79$) and a reliable Stroop interference effect (main effect of congruency: $F_{(1, 31)} = 32.53$, $p < 0.001$, $\eta_p^2 = 0.51$). Notably, the interaction between task type and congruency was significant ($F_{(1, 31)} = 8.62$, $p = 0.006$, $\eta_p^2 = 0.22$). Simple effect analysis revealed that, in the single-task condition, the RTs of incongruent trials were significantly slower ($M = 851.15$, $SE = 32.16$) than congruent trials ($M = 736.10$, $SE = 26.29$) ($p < 0.001$). However, in the dual-task condition, the RTs did not differ between incongruent trials ($M = 1073.04$, $SE = 39.73$) and congruent trials ($M = 1033.68$, $SE = 49.43$) ($p = 0.089$), indicating that the Stroop effect of RTs only occurred in single-task condition (Fig. 1).

2.2. ERP results

2.2.1. P1

Two-way repeated-measures ANOVA was conducted on the P1 component, revealing a significant main effect of task type ($F_{(1, 31)} = 29.92$, $p < 0.001$, $\eta_p^2 = 0.49$). Specifically, the P1 amplitude of the dual task ($M = 1.63$, $SE = 0.30$) was significantly greater than the single task ($M = 0.39$, $SE = 0.28$). However, neither the main effect of congruency ($F_{(1, 31)} = 0.00$, $p = 0.99$, $\eta_p^2 = 0.00$) nor the two-way interaction ($F_{(1, 31)} = 0.23$, $p = 0.63$, $\eta_p^2 = 0.007$) was significant (Fig. 2).

2.2.2. N450

Analysis of the N450 component showed the main effect of task type was significant ($F_{(1, 31)} = 23.79$, $p < 0.001$, $\eta_p^2 = 0.43$), resulting in greater N450 amplitude

in the single task (M = 1.90, SE = 0.33) compared to the dual task (M = 0.84, SE = 0.34). However, the main effect of current congruency ($F_{(1, 31)}$ = 1.60, p = 0.22, η_p^2 = 0.05) and the interaction ($F_{(1, 31)}$ = 0.02, p = 0.90, η_p^2 = 0.001) were not significant (Fig. 3A, B, C).

2.2.3. SP

For the SP component, two-way repeated-measures ANOVA showed the main effect of task type was significant ($F_{(1, 31)}$ = 14.54, p = 0.001, η_p^2 = 0.32) but the main effect of congruency was not ($F_{(1, 31)}$ =2.89, p = 0.10, η_p^2 = 0.09). Importantly, the interaction between congruency and task type was significant ($F_{(1, 31)}$ = 5.68, $p < 0.05$, η_p^2 = 0.16). Simple effect analysis showed that, in the single task, the SP amplitude in incongruent trials (M = 1.29, SE = 0.39) was significantly greater than in congruent trials (M = 0.70, SE = 0.30) (p = 0.009). On the contrary, in the dual task, the SP amplitude did not differ between congruent trials (M = 0.27, SE = 0.34) and incongruent trials (M = 0.22, SE = 0.37) (p = 0.98) (Fig. 3A, D, E).

2.3. MVPA results

Cluster-level permutation tests of the theta band indicated that only one cluster in 740-820 ms could significantly classify the Stroop effect of the single-task and dual-task (Fig. 4A). Regarding the beta band, tests showed a significant above-chance difference between the two task types from 920 ms to 1040 ms (Fig. 4C). However, no reliable decoding was observed between the two task types in the alpha band (Fig. 4B).

2.4. Time-Frequency results

2.4.1. Theta band

The two-way repeated-measures ANOVA on theta power revealed that the main effect of congruency was significant ($F_{(1, 31)} = 14.68$, $p = 0.001$, $\eta_p^2 = 0.32$), but the main effect of task type was not ($F_{(1, 31)} = 0.30$, $p = 0.59$, $\eta_p^2 = 0.01$). Notably, the interaction was significant ($F_{(1, 31)} = 7.71$, $p = 0.009$, $\eta_p^2 = 0.20$). Simple effect analysis showed that, in the dual task, the theta power did not differ between congruent trials ($M = 3.12$, $SE = 0.24$) and incongruent trials ($M = 3.27$, $SE = 0.24$) ($p = 0.63$). However, in the single task, the theta power was significantly higher in incongruent trials ($M = 4.00$, $SE = 0.32$) than in congruent trials ($M = 2.68$, $SE = 0.20$) ($p < 0.001$) (Fig. 5).

2.4.2. Beta band

Analysis of the beta power showed the main effect of task type ($F_{(1, 31)} = 34.55$, $p < 0.001$, $\eta_p^2 = 0.53$) and the main effect of congruency ($F_{(1, 31)} = 11.61$, $p = 0.002$, $\eta_p^2 = 0.27$) were both significant. Importantly, the interaction between task type and congruency reached a significant level ($F_{(1, 31)} = 15.64$, $p < 0.001$, $\eta_p^2 = 0.34$). Simple effect analysis revealed that, in the single-task condition, the beta power was significantly lower in the incongruent trials ($M = 0.53$, $SE = 0.06$) than in the congruent trials ($M = 0.80$, $SE = 0.08$) ($p < 0.001$). While no significant difference was found between them in the dual-task condition ($p = 0.40$) (Fig. 6).

2.5. RSA results

The RSA results showed that the interaction pattern in theta band significantly contributes to variation in the interaction pattern of response time (estimate = 0.17, *SE* = 0.05, t = 3.22, $p_{corrected}$ = 0.004). However, the correlation between the dissimilarity matrix of the SP (estimate = 0.02, *SE* = 0.05, t = 0.48, $p_{corrected}$ = 0.63) and theta (estimate = 0.10, *SE* = 0.05, t = 2.03, $p_{corrected}$ = 0.06) representation and the interaction pattern of response time was not significant (Fig. 7).

3. Discussion

The present study systematically investigated the dynamic neural mechanisms underlying the modulation of concurrent working memory task on Stroop conflict processing when the dimensions of memory information and distractors overlap. At first, we verified behaviorally that working memory processing eliminated the conflict effect. Specifically, in the single task, the response times of incongruent trials were significantly slower than congruent trials, but there was no significant difference between the two in the dual task. For the ERP results, no significant interaction was found in P1 or N450, but in SP. Namely, it showed that the incongruent trials evoked more positive SP than the congruent trials in the single task. While there was no difference between the two in the dual task. Moreover, MVPA results showed that only the theta power (740-820 ms) and the beta power (920-1040 ms) of conflict effect could successfully classify different task types. Further, in the corresponding time windows, we found that only in the single task, the incongruent trial induced greater theta power and smaller beta power than the congruent trial. Finally, RSA showed that only the interaction pattern in theta power correlated with response time.

All these results collectively suggested that, when the memorized information overlaps with the dimension of distractors, working memory processing modulates the late stage rather than early stage of Stroop conflict processing.

Behaviorally, we found that the Stroop interference effect was reduced under the dual-task condition, replicating previous findings (Kim et al., 2005; Luna et al., 2020; Park et al., 2007; Zhao et al., 2014). Consistent with the latest load theory (Murphy et al., 2016; Park et al., 2007), there are multiple resources, each with its own processing-specific, limited-capacity pool. Working memory load will tie up the limited resources necessary for distractor processing, diminishing the intensity of distractor processing, and thereby reducing their interference with the task. In our study, concurrent visual short-term working memory maintenance occupied the semantic resources required for distractor processing, resulting in the elimination of the Stroop effect. Interestingly, a previous study (Zhao et al., 2014) that reported a diminished Stroop interference effect employed the classic Chinese character Stroop task as well, but the working memory task involved memorizing meaningless visual shapes made from hand-drawn lines. This seems inconsistent with the load theory hypothesis, as the images appear to occupy spatial-related resources rather than overlapping with the distractor stimulus processing dimension. However, since Chinese characters are pictographs that require visual shape encoding and memory (Chaoran, 2019), they inherently occupy the same resources for processing Chinese characters as in our study. Additionally, this study suggested that the modulation effect of the working memory task on the typical Chinese character Stroop task was

relatively minor. We speculate that this is because graphic processing occupies lower-level resources related to the overall shape and spatial structure of Chinese characters (Zhang et al., 2020). In contrast, our study, which employed Chinese characters as the working memory load, could directly influence higher-level resources involved in semantic processing. Therefore, we believe that verbal working memory load can significantly modulate the Stroop effect. Overall, the improvement in conflict processing observed in our study is consistent with the core hypotheses of load theory based on multiple resources, paving the way for further exploration into the neural mechanisms behind this improvement.

The ERP findings indicated that the working memory task influenced only the SP component, which reflects the process of conflict resolution. Consistent with most research, our study showed that the SP amplitude is more positive in conflict situations (Heidlmayr et al., 2020; Zhao et al., 2015). Crucially, our study found that verbal working memory load eliminated the difference in SP between congruent and incongruent trials, indicating that conflict resolution did not occur in the dual-task condition. Furthermore, Some studies have suggested that N450 and SP are related to stimulus conflict (or semantic conflict) and response conflict, respectively (Coderre et al., 2011; West et al., 2005; Zhao et al., 2015). Therefore, this result may imply that participants neither encountered stimulus conflict nor response conflict in the dual-task condition. Additionally, our study did not find any differences in P1 and N450 between the different trial types. For P1, most studies indicate that Stroop interference occurs only in the later stages of response selection, rather than during the sensory

input processing stage (David et al., 2011; Di Russo & Bianco, 2023). For N450, our previous research shows that semantic conflict in the Stroop task only appears in the early practice stages, and the manual Stroop task should include only “pure” response conflict (Chen et al., 2013). Therefore, due to the practice effect, the semantic conflict represented by N450 may have disappeared in this study. Generally, the overall ERP results suggest that working memory influences the later stage of response conflict resolution, while not influencing the early stage of perceptual processing and semantic encoding.

In addition to the ERP results, the MVPA results from time-frequency also provide supportive evidence that working memory modulates Stroop conflict processing in the later stage. First, in line with the previous study (Zhao et al., 2014), there are no continuous time periods in which alpha activities (incongruency minus congruency) can successfully discriminate the single-task and dual-task. Alpha is regarded as an indicator of top-down attentional modulation, with an increase in alpha reflecting the inhibition of distractor input (Van Diepen et al., 2019; Zhou et al., 2023), implying that the patterns of attentional adjustment are similar across different task types in our study. This finding may be related to the attentional rejection template (Wen et al., 2022). In the Sternberg task, participants are required to remember only seven Chinese characters and reject the others, which is similar to the attention template used for rejecting characters in the Stroop task. Second, the different task types can be successfully discriminated by late theta activity after the stimulus presentation (740-820 ms). Similarly, previous research has found that

current working memory leads to smaller differences in theta activity (400-1000 ms) between incongruent and neutral trials (Zhao et al., 2014). According to the framework of event coding theory (TEC), late theta may represent the process of stimulus-response binding or mapping (Beste et al., 2023; Wendiggensen et al., 2023). And this has been demonstrated in several empirical experiments. For example, theta is thought to be involved in adjusting the processing of stimulus information to correspond with appropriate responses (Cavanagh et al., 2009). In line with this opinion, about -200 to 0 ms before a response, higher theta activity is observed in high-conflict conditions compared to low-conflict conditions (Cohen & Donner, 2013). Accordingly, working memory may eliminate the Stroop effect by influencing the stimulus-response mapping process. Lastly, the present study also shows that beta activity between 920-1040 ms after stimulus presentation can successfully discriminate between the two task types. Beta activity is often thought to be associated with motor priming. Specifically, it decreases at the onset of movement (Jenkinson & Brown, 2011), but increases during holding a static status (Baker et al., 2001). Since response button selection definitely occurs after conflict resolution and is a late motor adjustment according to the stimulus, this result suggests that working memory may also influence the response output stage of Stroop conflict processing.

The RSA results further reveal that the neural activity pattern of theta is most similar to the behavioral Stroop effect modulation pattern. This result can be interpreted from the standpoint of neural efficiency, suggesting that a reduction in activation patterns reflects greater neural efficiency (Rypma et al., 2006). Therefore,

we speculate that the core reason for the disappearance of the behavioral Stroop effect under the dual-task condition is that, compared to congruent trials, neural activation in theta decreases and response speed increases in incongruent trials (Fig. 1 and Fig. 5C). Moreover, this result aligns with many studies that have found theta can predict reaction times (Kaiser & Schütz-Bosbach, 2021; Senoussi et al., 2022). However, although SP and beta exhibited interaction effects in the data patterns, they may not be the core indicators directly determining the behavioral modulation effect. SP, as an ERP component, contains multiple oscillatory bands, indicating several parallel brain processes (Brilliant et al., 2024). Beta, as a general response-related indicator, may not be directly linked to conflict processing. Combined with the MVPA decoding results indicating that the beta band (920-1040 ms) follows the theta band (740-820 ms), we speculate that changes in beta bands may be influenced by theta bands, thereby indirectly influencing the behavioral Stroop effect. Overall, when the dimensions of working memory load overlap with those of distractor stimuli, individuals do not need to engage in conflict resolution. Specifically, the memory information occupies the resources for the late-stage stimulus-response mapping of the distractors, weakening the mapping of distractors to incorrect responses, and subsequently inhibiting the response output of the distractors, resulting in the disappearance of response conflict.

In summary, this study demonstrated that the concurrent working memory task can eliminate Stroop conflict through disrupting stimulus-response mapping. The results indicated that concurrent working memory load influenced the late stage

related to stimulus-response mapping and response selection processes, indexed by SP, late theta band, and beta band; while it did not influence the early stage associated with perceptual processing and attention adjustment, indexed by P1 and alpha band. RSA further identified theta as the neural indicator directly associated with the behavioral modulation pattern. These findings suggested that when the working memory load overlaps with the dimension of distractor stimuli, it occupies the resources for the stimulus-response mapping of the distractor, weakening the stronger response tendency of the distractor, and ultimately leading to the disappearance of response conflict. Accordingly, the present study comprehensively characterized the dynamic neural mechanisms by which working memory modulates Stroop conflict processing, further deepening our understanding of the mechanisms underlying conflict generation.

4. Materials and methods

4.1. Participants

Using G*Power software (Faul et al., 2007), we calculated the sample size for the experiment. The power analysis (power ≥ 0.9) on within-factors designs, assuming a moderate effect size of 0.25, indicated a sample size of 30. We recruited 34 healthy subjects (17 females; age: 21.38 ± 1.92 years) through advertisements. Two subjects were excluded from further analyses due to excessive EEG artifacts. Finally, a total of 32 subjects (16 females; age: 21.44 ± 1.97 years) remained for behavioral and EEG analyses. All participants were right-handed, had normal or corrected-to-normal

vision and normal color perception assessed by the Ishihara Color Test, and reported no history of neurologic or psychiatric disease. They all signed written informed consent before the experiment. All procedures were conducted in accordance with the principles of the Declaration of Helsinki and its later amendments and were approved by the Human Research Human Ethics Committee of the Shanghai University of Sport.

4.2. Apparatus and Stimuli

Participants were instructed to perform experiments in a soundproof room. The experimental stimuli were presented on a 19-inch color monitor (resolution 1920 × 1080, refresh rate 60 Hz) with a viewing distance of approximately 65 cm. Stimulus presentation and response recording were controlled by a Microsoft PC running Matlab (Mathworks, Inc.) with Psychophysics Toolbox extensions (Brainard, 1997; Pelli, 1997).

The experiment employed the single task (the classical manual Stroop task) and the dual task (the Sternberg working memory task combined with the Stroop task). The Stroop task stimuli consisted of four Chinese words: “红” (red, RGB: 255, 0, 0), “绿” (green, RGB: 0, 255, 0), “蓝” (blue, RGB: 0, 0, 255), and “黄” (yellow, RGB: 255, 255, 0). They were presented in the semantically corresponding font color (congruent trials) or a different font color (incongruent trials) in the center of a black background (visual angle, ~1.15×1.15°). The Sternberg working memory task involved seven Chinese characters chosen randomly among 14 familiar Chinese

characters: “人” (human), “刀” (knife), “大” (big), “水” (water), “天” (heaven), “口” (mouth), “月” (moon), “立” (stand), “山” (mountain), “上” (up), “手” (hand), “石” (stone), “女” (woman), and “火” (fire) (Zhao et al., 2010). They were equally spaced on a horizontal row at the center of the display (visual angle for each character, ~1.15×1.15°).

4.3. Procedure

For the dual task (Fig.8A), the subjects were required to memorize seven Chinese characters in anticipation of a recognition test at the end of the trial. Each trial began with a white fixation point for a random duration from 400 to 600 ms, followed by seven white Chinese characters that required memorization for 2000 ms. After a jittered 800-1200 ms fixation point, participants performed a Stroop task in which the color of the words were identified as quickly as possible by pressing the corresponding button (“F” with the left index finger, “D” with the left middle finger, “J” with the right index finger, and “K” with the right middle finger), while attempting to ignore the task-irrelevant semantic meaning. The display for the words remained on the screen until a response was made. After the Stroop task, a fixation point was randomly presented for 400-600 ms, and terminated by the appearance of a probe character, to which the subject had to determine if the character was part of their memorized list of items. During 50% of the trials, the probe letter was included as part of the memorized set. Participants were asked to answer by pressing one of two response buttons (“S” with the left ring finger and “L” with the left ring finger). All response buttons in this experiment were counterbalanced across subjects. After a

response was given, the intertrial interval was randomized between 600 and 1000 ms until the onset of the next trial. For the single task (Fig.8B), subjects were only required to complete the individual Stroop task. Each block alternated between single and dual tasks in an ABAB fashion, and the task type in the first block was counterbalanced across participants. Participants were permitted to participate in the formal experiment when their average error rate was below 15%. The formal experiment included six blocks, totaling 144 trials, with an equal distribution of 50% congruent and 50% incongruent trials presented randomly in each block. The entire experiment lasted for around 30 minutes.

4.4. EEG recording and preprocessing

EEG data were recorded using standard 64 in-cap Ag/AgCl electrodes, following the extended international 10-20 system (Brain Products GmbH, Germany; pass band, 0.01-100 Hz; sampling rate, 1000 Hz). Vertical and horizontal electrooculograms (EOGs) were recorded from below the left eye and outer canthus of the right eye, respectively. The FCz served as an online reference. The impedance of all electrodes was maintained below 5 kΩ during the entire recording process.

The offline EEG data were preprocessed by EEGLAB V2023.0 (Delorme & Makeig, 2004) and custom scripts in MATLAB 2021a. First, the continuous data was down-sampled from the original sampling rate of 1000 Hz to 500 Hz. Then, the data were filtered with a 30 Hz low-pass filter and a 0.1 Hz high-pass filter. After that, we re-referenced the data to the average activity of all scalp channels and manually

inspected the data to remove obvious artifacts. Subsequently, we carried out an independent component analysis (ICA, infomax algorithm) and thereby identified and manually removed artifacts such as eyeblinks, horizontal eye movements, heart, muscle, and line noise. As a next step, the data was segmented based on the trial type (single-task congruent vs. single-task incongruent vs. dual-task congruent vs. dual-task incongruent) and was time-locked to the Stroop stimulus onset. Continuous EEG data were epoched from −200 to 1000 ms relative to word onset, with a baseline correction applied using the 200 ms pre-stimulus interval. Finally, trials with amplitude values exceeding ±100 μV at any electrode were rejected.

4.5. Data analysis

4.5.1. Behavioral analysis

Only trials that were correct in both the memory task and the Stroop task were included in all subsequent analyses. In addition, trials in which response times (RTs) deviated by more than three standard deviations from the condition mean were excluded from behavioral analyses. We performed repeated-measures analysis of variance (ANOVA) with Greenhouse-Geisser correction if needed, in which the within-subject factors were congruency (congruent, incongruent) and task type (single task, dual task). Adjustments for multiple comparisons were realized using Bonferroni correction.

4.5.2. ERP analysis

Considering previous studies (Coderre et al., 2011; Xu et al., 2024; Zivony &

Lamy, 2022), P1 was calculated using a time window of 40 ms (110-150 ms) at bilateral occipito-parietal electrodes (PO3, PO4, PO7, PO8, P7, P8). N450 was computed using a time window of 150 ms (350-500 ms) at centro-parietal electrodes (Cz, CPz, Pz). SP was scored as the mean amplitude at centro-parietal electrodes (Cz, CPz, Pz) during a time window of 300 ms (650-950 ms).

4.5.3. Multivariate pattern analysis

Our multivariate pattern analysis was based on support vector machine (SVM), a supervised machine learning method that operated on labeled samples. A binary label with 1 for the single task and -1 for the dual task was used in this study. The classification process at a given time point included a training phase and a testing phase. During the training step, the SVM would find a decision boundary that separated the samples in the input features using class labels. Next, the trained classifier is used to predict the class labels of new examples. For the spectral MVPA, we defined three frequency regions of interest (F-ROIs): theta (4-7 Hz), alpha (8-13 Hz), and beta (14-25 Hz). Then, three spatial regions of interest (S-ROIs) were chosen: fronto-central (Fz, FCz, Cz), occipital-parietal (POz, Oz, PO3, PO4, PO7, PO8, O1, O2) and central (C3, CP3, Cz, CP4, C4) to measure theta, alpha and beta power, respectively (Zhao et al., 2015; Li et al., 2021). For each frequency band, the selected features were the power difference between congruent and incongruent trials in the single task and dual task in every 20 ms of each ROI (See “Time-frequency analysis” section for the power transformation method). All data were normalized and mapped to the range [-1, 1] within each class to mitigate scale effects.

A linear kernel SVM was chosen and trained through the LIBSVM toolbox (Chang & Lin, 2011). The linear SVM has only one parameter C that determines the trade-off between allowing misclassifications and training error minimization. The functions were as follows:

$$K(X_i, X_j) = X_i^T X_j$$

$$\min \frac{1}{2} \|\omega\|^2 + C \sum_{i=1}^{m} \xi(i)$$

A classifier was trained and tested at each time point by using a 5-fold cross-validation procedure. Trials were randomly divided into 5 equal-sized folds. Then, a leave-one-out procedure was run in which the classifier was trained on 4-folds and tested on the remaining fold. In this case, different C values were tried within a certain range to find the best cross-validation accuracy (or the smallest value if there were more than one). We set the range of C values to base 2, and the exponent range to [10, 10] with a step size of 0.2. Here, accuracy was used to quantify the performance of the classifier based on the results of cross-validation.

For statistical analyses, a nonparametric statistical test based on the cluster-level permutation was implemented to deal with multiple comparisons while maintaining strict control of the false-alarm rate (Maris & Oostenveld, 2007). In detail, t-tests against chance level (acc = 0.5) were carried out at each data point to obtain the statistic values. Statistical values with p-values < 0.01 were clustered together by summing their statistic values. The cluster alpha was set to 0.01 to reduce the likelihood of large clusters spanning the entire dataset (Mensen & Khatami, 2013).

Additionally, to avoid using extremely transient intervals that may not capture meaningful psychological phenomena, we specified that at least two significant time points formed a cluster. Then, we permuted the data for 1000 times by randomly swapping condition labels to obtain a permutation distribution of the maximum cluster-level statistic under the null hypothesis of no condition difference. If there was any cluster with its real statistic larger than the threshold, we rejected the null hypothesis and concluded that there was a significant difference.

4.5.4. Time-frequency analysis

To avoid edge artifacts, EEG data were re-epoched from -1000 ms to 2000 ms relative to stimulus onset. EEG data were converted into time-frequency domain data using continuous wavelet transform in Letswave Software (https://www.letswave .org/; Mouraux & Iannetti, 2008). The cmor1-1.5 was chosen as the mother wavelet function for the time-frequency representations ranging from 1 to 30 Hz with a step size of 0.29 Hz. The single-trial time-frequency representation was obtained after wavelet transform, and they were then averaged throughout all trials per condition. The baseline normalizations were performed at each time point for each frequency using an event-related spectral perturbation (ERSP) transformation [$ER_{t,f}\% = [A_{t,f} - R_f]/R_f$] (Pfurtscheller & Lopes da Silva, 1999). A 400-200 ms pre-stimulus time window was selected as the baseline time window. For the statistical test, we only analyzed the frequency bands and corresponding time windows that could successfully classify different tasks in MVPA, namely theta (740-820 ms) and beta (920-1040 ms).

4.5.5. Representational similarity analysis

Our RSA analysis aimed to explore the correlation between neural interaction patterns and behavioral interaction patterns. First, we extracted data that could reflect interaction patterns, namely Stroop effect differences between single-task and dual-task conditions based on the subject-level in RT, SP, theta, and beta. Prior to analysis, data were normalized by z-scoring the values across all subjects. We then constructed Representational Dissimilarity Matrices (RDMs) measuring the geometrical distances between all subjects, yielding 32 × 32 symmetrical matrices. Here, Euclidean distance was employed to measure the distance between subjects (Edelman, 1998). Finally, we fitted a linear regression with the neural RDMs as regressors and the behavioral RDM as the dependent variable to test which neural RDMs could predict behavioral RDMs. *P*-values were corrected by the false discovery rate.

Data availability

Data and codes presented in this work are available at: https://osf.io/89bpz/.

Author Contributions

Yafen Li: Conceptualization, Data curation, Methodology, Investigation, Visualization, Writing - original draft. Yixuan Lin: Methodology, Visualization, Writing - review & editing. Qing Li: Conceptualization, Methodology, Validation. Yongqiang Chen: Methodology, Validation. Zhifang Li: Methodology, Validation. Antao Chen: Conceptualization, Supervision, Writing - review & editing.

Funding information

This work was supported by grants from the National Natural Science Foundation of China (32371105).

Competing interests

The authors declare that they have no competing interests.

References

Algom, D., Fitousi, D., & Chajut, E. (2022). Can the Stroop effect serve as the gold standard of conflict monitoring and control? A conceptual critique. *Memory & Cognition*, *50*(5), 883–897. https://doi.org/10.3758/s13421-021-01251-5

Allen, M., Poggiali, D., Whitaker, K., Marshall, T. R., van Langen, J., & Kievit, R. A. (2021). Raincloud plots: A multi-platform tool for robust data visualization. *Wellcome Open Research*, *4*, 63. https://doi.org/10.12688/wellcomeopenres.15191.2

Arakaki, X., Hung, S.-M., Rochart, R., Fonteh, A. N., & Harrington, M. G. (2022). Alpha desynchronization during Stroop test unmasks cognitively healthy individuals with abnormal CSF Amyloid/Tau. *Neurobiology of Aging*, *112*, 87–101. https://doi.org/10.1016/j.neurobiolaging.2021.11.009

Augustinova, M., Parris, B. A., & Ferrand, L. (2019). The Loci of Stroop Interference and Facilitation Effects With Manual and Vocal Responses. *Frontiers in Psychology*, *10*. https://www.frontiersin.org/articles/10.3389/fpsyg.2019.01786

Baddeley, A. (2012). Working Memory: Theories, Models, and Controversies. *Annual Review of Psychology*, *63*(Volume 63, 2012), 1–29. https://doi.org/10.1146/annurev-psych-120710-100422

Baker, S. N., Spinks, R., Jackson, A., & Lemon, R. N. (2001). Synchronization in Monkey Motor Cortex During a Precision Grip Task. I. Task-Dependent Modulation in Single-Unit Synchrony. *Journal of Neurophysiology*, *85*(2), 869–885. https://doi.org/10.1152/jn.2001.85.2.869

Banich, M. T. (2019). The Stroop Effect Occurs at Multiple Points Along a Cascade of Control: Evidence From Cognitive Neuroscience Approaches. *Frontiers in Psychology*, *10*, 2164. https://doi.org/10.3389/fpsyg.2019.02164

Beste, C., Münchau, A., & Frings, C. (2023). Towards a systematization of brain oscillatory activity in actions. *Communications Biology*, *6*(1), Article 1. https://doi.org/10.1038/s42003-023-04531-9

Böttcher, A., Wilken, S., Adelhöfer, N., Raab, M., Hoffmann, S., & Beste, C. (2023). A dissociable functional relevance of theta- and beta-band activities during complex sensorimotor integration. *Cerebral Cortex*, *33*(14), 9154–9164. https://doi.org/10.1093/cercor/bhad191

Brainard, D. H. (1997). The Psychophysics Toolbox. *Spatial Vision*, *10*(4), 433–436. https://doi.org/10.1163/156856897X00357

Brilliant, Yaar-Soffer, Y., Herrmann, C. S., Henkin, Y., & Kral, A. (2024). Theta and alpha oscillatory signatures of auditory sensory and cognitive loads during complex listening. *NeuroImage*, *289*, 120546. https://doi.org/10.1016/j.neuroimage.2024.120546

Brockhoff, L., Schindler, S., Bruchmann, M., & Straube, T. (2022). Effects of perceptual and working memory load on brain responses to task-irrelevant stimuli: Review and implications for future research. *Neuroscience & Biobehavioral Reviews*, *135*, 104580. https://doi.org/10.1016/j.neubiorev.2022.104580

Bugg, J. M., & Crump, M. J. C. (2012). In Support of a Distinction between Voluntary

and Stimulus-Driven Control: A Review of the Literature on Proportion Congruent Effects. *Frontiers in Psychology*, *3*. https://doi.org/10.3389/fpsyg.2012.00367

Cavanagh, J. F., Cohen, M. X., & Allen, J. J. B. (2009). Prelude to and Resolution of an Error: EEG Phase Synchrony Reveals Cognitive Control Dynamics during Action Monitoring. *Journal of Neuroscience*, *29*(1), 98–105. https://doi.org/10.1523/JNEUROSCI.4137-08.2009

Cavanagh, J. F., & Frank, M. J. (2014). Frontal theta as a mechanism for cognitive control. *Trends in Cognitive Sciences*, *18*(8), 414–421. https://doi.org/10.1016/j.tics.2014.04.012

Chang, C.-C., & Lin, C.-J. (2011). LIBSVM: A library for support vector machines. *ACM Transactions on Intelligent Systems and Technology*, *2*(3), 27:1-27:27. https://doi.org/10.1145/1961189.1961199

Chaoran, Y. (2019). Pictographs of gastroparesis in Chinese characters. *Neurogastroenterology and Motility*, *31*(8). https://doi.org/10.1111/NMO.13660

Chen, Z., Lei, X., Ding, C., Li, H., & Chen, A. (2013). The neural mechanisms of semantic and response conflicts: An fMRI study of practice-related effects in the Stroop task. *NeuroImage*, *66*, 577–584. https://doi.org/10.1016/j.neuroimage.2012.10.028

Chung, R. S., Cavaleri, J., Sundaram, S., Gilbert, Z. D., Del Campo-Vera, R. M., Leonor, A., Tang, A. M., Chen, K.-H., Sebastian, R., Shao, A., Kammen, A., Tabarsi, E., Gogia, A. S., Mason, X., Heck, C., Liu, C. Y., Kellis, S. S., & Lee, B.

(2024). Understanding the human conflict processing network: A review of the literature on direct neural recordings during performance of a modified stroop task. *Neuroscience Research*. https://doi.org/10.1016/j.neures.2024.03.006

Coderre, E., Conklin, K., & van Heuven, W. J. B. (2011). Electrophysiological measures of conflict detection and resolution in the Stroop task. *Brain Research*, *1413*, 51–59. https://doi.org/10.1016/j.brainres.2011.07.017

Cohen, M. X., & Donner, T. H. (2013). Midfrontal conflict-related theta-band power reflects neural oscillations that predict behavior. *Journal of Neurophysiology*, *110*(12), 2752–2763. https://doi.org/10.1152/jn.00479.2013

David, I. A., Volchan, E., Vila, J., Keil, A., De Oliveira, L., Faria-Júnior, A. J. P., Perakakis, P., Dias, E. C., Mocaiber, I., Pereira, M. G., & Machado-Pinheiro, W. (2011). Stroop matching task: Role of feature selection and temporal modulation. *Experimental Brain Research*, *208*(4), 595–605. https://doi.org/10.1007/s00221-010-2507-9

Delorme, A., & Makeig, S. (2004). EEGLAB: An open source toolbox for analysis of single-trial EEG dynamics including independent component analysis. *Journal of Neuroscience Methods*, *134*(1), 9–21. https://doi.org/10.1016/j.jneumeth.2003.10.009

Di Russo, F., & Bianco, V. (2023). Time Course of Reactive Brain Activities during a Stroop Color-Word Task: Evidence of Specific Facilitation and Interference Effects. *Brain Sciences*, *13*(7), Article 7. https://doi.org/10.3390/brainsci13070982

Donohue, S. E., Appelbaum, L. G., McKay, C. C., & Woldorff, M. G. (2016). The neural dynamics of stimulus and response conflict processing as a function of response complexity and task demands. *Neuropsychologia*, *84*, 14–28. https://doi.org/10.1016/j.neuropsychologia.2016.01.035

Edelman, S. (1998). Representation is representation of similarities. *The Behavioral and Brain Sciences*, *21*(4), 449–467; discussion 467-498. https://doi.org/10.1017/s0140525x98001253

Faul, F., Erdfelder, E., Lang, A.-G., & Buchner, A. (2007). G*Power 3: A flexible statistical power analysis program for the social, behavioral, and biomedical sciences. *Behavior Research Methods*, *39*(2), 175–191. https://doi.org/10.3758/BF03193146

Freund, M. C., Etzel, J. A., & Braver, T. S. (2021). Neural Coding of Cognitive Control: The Representational Similarity Analysis Approach. *Trends in Cognitive Sciences*, *25*(7), 622–638. https://doi.org/10.1016/j.tics.2021.03.011

Friehs, M. A., Klaus, J., Singh, T., Frings, C., & Hartwigsen, G. (2020). Perturbation of the right prefrontal cortex disrupts interference control. *NeuroImage*, *222*, 117279. https://doi.org/10.1016/j.neuroimage.2020.117279

Haciahmet, C. C., Frings, C., Beste, C., Münchau, A., & Pastötter, B. (2023). Posterior delta/theta EEG activity as an early signal of Stroop conflict detection. *Psychophysiology*, *60*(3), e14195. https://doi.org/10.1111/psyp.14195

Hallenbeck, G. E., Sprague, T. C., Rahmati, M., Sreenivasan, K. K., & Curtis, C. E. (2021). Working memory representations in visual cortex mediate distraction

effects. *Nature Communications*, *12*(1), 4714. https://doi.org/10.1038/s41467-021-24973-1

Heidlmayr, K., Kihlstedt, M., & Isel, F. (2020). A review on the electroencephalography markers of Stroop executive control processes. *Brain and Cognition*, *146*, 105637. https://doi.org/10.1016/j.bandc.2020.105637

Itthipuripat, S., Deering, S., & Serences, J. (2019). When Conflict Cannot be Avoided: Relative Contributions of Early Selection and Frontal Executive Control in Mitigating Stroop Conflict. *Cerebral Cortex*, *29*, 1–12. https://doi.org/10.1093/cercor/bhz042

Jenkinson, N., & Brown, P. (2011). New insights into the relationship between dopamine, beta oscillations and motor function. *Trends in Neurosciences*, *34*(12), 611–618. https://doi.org/10.1016/j.tins.2011.09.003

Kaiser, J., & Schütz-Bosbach, S. (2021). Motor Interference, But Not Sensory Interference, Increases Midfrontal Theta Activity and Brain Synchronization during Reactive Control. *The Journal of Neuroscience*, *41*(8), 1788–1801. https://doi.org/10.1523/JNEUROSCI.1682-20.2020

Kim, S.-Y., Kim, M.-S., & Chun, M. M. (2005). Concurrent working memory load can reduce distraction. *Proceedings of the National Academy of Sciences of the United States of America*, *102*(45), 16524–16529. https://doi.org/10.1073/pnas.0505454102

Klimesch, W., Hanslmayr, S., Sauseng, P., Gruber, W. R., & Doppelmayr, M. (2007). P1 and Traveling Alpha Waves: Evidence for Evoked Oscillations. *Journal of*

Neurophysiology, *97*(2), 1311–1318. https://doi.org/10.1152/jn.00876.2006

Kriegeskorte, N., & Kievit, R. A. (2013). Representational geometry: Integrating cognition, computation, and the brain. *Trends in Cognitive Sciences*, *17*(8), 401–412. https://doi.org/10.1016/j.tics.2013.06.007

Li, Q., Hu, N., Li, Y., Long, Q., Gu, Y., Tang, Y., & Chen, A. (2021). Error-induced adaptability: Behavioral and neural dynamics of response-stimulus interval modulations on posterror slowing. *Journal of Experimental Psychology: General*, *150*(5), 851–863. https://doi.org/10.1037/xge0000978

Li, Q., Yin, S., Wang, J., Zhang, M., Li, Z., Chen, X., & Chen, A. (2023). Not all errors are created equal: Decoding the error-processing mechanisms using alpha oscillations. *Cerebral Cortex*, bhad102. https://doi.org/10.1093/cercor/bhad102

Lin, Y., Li, Q., & Chen, A. (2023). The causal mechanisms underlying analogical reasoning performance improvement by executive attention intervention. *Human Brain Mapping*, *44*(8), 3241–3253. https://doi.org/10.1002/hbm.26278

Luna, F. G., Telga, M., Vadillo, M. A., & Lupiáñez, J. (2020). Concurrent working memory load may increase or reduce cognitive interference depending on the attentional set. *Journal of Experimental Psychology: Human Perception and Performance*, *46*(7), 667–680. https://doi.org/10.1037/xhp0000740

Maris, E., & Oostenveld, R. (2007). Nonparametric statistical testing of EEG- and MEG-data. *Journal of Neuroscience Methods*, *164*(1), 177–190. https://doi.org/10.1016/j.jneumeth.2007.03.024

Meier, T. B., Desphande, A. S., Vergun, S., Nair, V. A., Song, J., Biswal, B. B.,

Meyerand, M. E., Birn, R. M., & Prabhakaran, V. (2012). Support vector machine classification and characterization of age-related reorganization of functional brain networks. *NeuroImage*, *60*(1), 601–613. https://doi.org/10.1016/j.neuroimage.2011.12.052

Mensen, A., & Khatami, R. (2013). Advanced EEG analysis using threshold-free cluster-enhancement and non-parametric statistics. *NeuroImage*, *67*, 111–118. https://doi.org/10.1016/j.neuroimage.2012.10.027

Mouraux, A., & Iannetti, G. D. (2008). Across-trial averaging of event-related EEG responses and beyond. *Magnetic Resonance Imaging*, *26*(7), 1041–1054. https://doi.org/10.1016/j.mri.2008.01.011

Murphy, G., Groeger, J. A., & Greene, C. M. (2016). Twenty years of load theory—Where are we now, and where should we go next? *Psychonomic Bulletin & Review*, *23*(5), 1316–1340. https://doi.org/10.3758/s13423-015-0982-5

Okayasu, M., Inukai, T., Tanaka, D., Tsumura, K., Shintaki, R., Takeda, M., Nakahara, K., & Jimura, K. (2023). The Stroop effect involves an excitatory–inhibitory fronto-cerebellar loop. *Nature Communications*, *14*(1), Article 1. https://doi.org/10.1038/s41467-022-35397-w

Park, S., Kim, M.-S., & Chun, M. (2007). Concurrent Working Memory Load Can Facilitate Selective Attention: Evidence for Specialized Load. *Journal of Experimental Psychology. Human Perception and Performance*, *33*, 1062–1075. https://doi.org/10.1037/0096-1523.33.5.1062

Parris, B., Hasshim, N., Wadsley, M., Augustinova, M., & Ferrand, L. (2022). The loci

of Stroop effects: A critical review of methods and evidence for levels of processing contributing to color-word Stroop effects and the implications for the loci of attentional selection. *Psychological Research*, *86*, 1029–1053. https://doi.org/10.1007/s00426-021-01554-x

Pelli, D. G. (1997). The VideoToolbox software for visual psychophysics: Transforming numbers into movies. *Spatial Vision*, *10*(4), 437–442. https://doi.org/10.1163/156856897X00366

Pfurtscheller, G., & Lopes da Silva, F. H. (1999). Event-related EEG/MEG synchronization and desynchronization: Basic principles. *Clinical Neurophysiology: Official Journal of the International Federation of Clinical Neurophysiology*, *110*(11), 1842–1857. https://doi.org/10.1016/s1388-2457(99)00141-8

Rypma, B., Berger, J. S., Prabhakaran, V., Martin Bly, B., Kimberg, D. Y., Biswal, B. B., & D'Esposito, M. (2006). Neural correlates of cognitive efficiency. *NeuroImage*, *33*(3), 969–979. https://doi.org/10.1016/j.neuroimage.2006.05.065

Schmidt, J. R. (2019). Evidence against conflict monitoring and adaptation: An updated review. *Psychonomic Bulletin & Review*, *26*(3), 753–771. https://doi.org/10.3758/s13423-018-1520-z

Senoussi, M., Verbeke, P., Desender, K., De Loof, E., Talsma, D., & Verguts, T. (2022). Theta oscillations shift towards optimal frequency for cognitive control. *Nature Human Behaviour*, *6*(7), Article 7. https://doi.org/10.1038/s41562-022-01335-5

Stroop, J. R. (1935). Studies of interference in serial verbal reactions. *Journal of Experimental Psychology*, *18*(6), 643–662. https://doi.org/10.1037/h0054651

Tafuro, A., Ambrosini, E., Puccioni, O., & Vallesi, A. (2019). Brain oscillations in cognitive control: A cross-sectional study with a spatial stroop task. *Neuropsychologia*, *133*, 107190. https://doi.org/10.1016/j.neuropsychologia.2019.107190

Van Diepen, R. M., Foxe, J. J., & Mazaheri, A. (2019). The functional role of alpha-band activity in attentional processing: The current zeitgeist and future outlook. *Current Opinion in Psychology*, *29*, 229–238. https://doi.org/10.1016/j.copsyc.2019.03.015

Viviani, G., Visalli, A., Montefinese, M., Vallesi, A., & Ambrosini, E. (2023). The Stroop legacy: A cautionary tale on methodological issues and a proposed spatial solution. *Behavior Research Methods*. https://doi.org/10.3758/s13428-023-02215-0

Vo, K. D., Siqi-Liu, A., Chaire, A., Li, S., Demeter, E., Egner, T., & Woldorff, M. G. (2021). Neural Dynamics of Conflict Control in Working Memory. *Journal of Cognitive Neuroscience*, *33*(10), 2079–2092. https://doi.org/10.1162/jocn_a_01744

Wen, W., Huang, Z., Hou, Y., & Li, S. (2022). Tracking Neural Markers of Template Formation and Implementation in Attentional Inhibition under Different Distractor Consistency. *Journal of Neuroscience*, *42*(24), 4927–4936. https://doi.org/10.1523/JNEUROSCI.1705-21.2022

Wendiggensen, P., Adelhöfer, N., Jamous, R., Mückschel, M., Takacs, A., Frings, C., Münchau, A., & Beste, C. (2022). Processing of embedded response plans is modulated by an interplay of frontoparietal theta and beta activity. *Journal of Neurophysiology*, *128*(3), 543–555. https://doi.org/10.1152/jn.00537.2021

Wendiggensen, P., Prochnow, A., Pscherer, C., Münchau, A., Frings, C., & Beste, C. (2023). Interplay between alpha and theta band activity enables management of perception-action representations for goal-directed behavior. *Communications Biology*, *6*(1), Article 1. https://doi.org/10.1038/s42003-023-04878-z

West, R., Jakubek, K., Wymbs, N., Perry, M., & Moore, K. (2005). Neural correlates of conflict processing. *Experimental Brain Research*, *167*(1), 38–48. https://doi.org/10.1007/s00221-005-2366-y

Wolff, M. J., Kandemir, G., Stokes, M. G., & Akyürek, E. G. (2020). Unimodal and Bimodal Access to Sensory Working Memories by Auditory and Visual Impulses. *Journal of Neuroscience*, *40*(3), 671–681. https://doi.org/10.1523/JNEUROSCI.1194-19.2019

Xu, H., Yang, G., Wu, H., Xiao, J., Li, Q., & Liu, X. (2024). Distinct mechanisms underlying cross-modal semantic conflict and response conflict processing. *Cerebral Cortex*, *34*(2), bhad539. https://doi.org/10.1093/cercor/bhad539

Yang, G., Wu, H., Li, Q., Liu, X., Fu, Z., & Jiang, J. (2023). Conflicts are represented in a cognitive space to reconcile domain-general and domain-specific cognitive control. *eLife*, *12*. https://doi.org/10.7554/eLife.87126.1

Yu, B., Wang, X., Ma, L., Li, L., & Li, H. (2015). The Complex Pre-Execution Stage

of Auditory Cognitive Control: ERPs Evidence from Stroop Tasks. *PLOS ONE*, *10*(9), e0137649. https://doi.org/10.1371/journal.pone.0137649

Zhang, X., Yang, S., & Jiang, M. (2020). Rapid implicit extraction of abstract orthographic patterns of Chinese characters during reading. *PLOS ONE*, *15*(2), e0229590. https://doi.org/10.1371/journal.pone.0229590

Zhao, J., Liang, W.-K., Juan, C.-H., Wang, L., Wang, S., & Zhu, Z. (2015). Dissociated stimulus and response conflict effect in the Stroop task: Evidence from evoked brain potentials and brain oscillations. *Biological Psychology*, *104*, 130–138. https://doi.org/10.1016/j.biopsycho.2014.12.001

Zhao, X., Chen, A., & West, R. (2010). The influence of working memory load on the Simon effect. *Psychonomic Bulletin & Review*, *17*(5), 687–692. https://doi.org/10.3758/PBR.17.5.687

Zhao, Y., Tang, D., Hu, L., Zhang, L., Hitchman, G., Wang, L., & Chen, A. (2014). Concurrent working memory task decreases the Stroop interference effect as indexed by the decreased theta oscillations. *Neuroscience*, *262*, 92–106. https://doi.org/10.1016/j.neuroscience.2013.12.052

Zhou, Y. J., Ramchandran, A., & Haegens, S. (2023). Alpha oscillations protect working memory against distracters in a modality-specific way. *NeuroImage*, *278*, 120290. https://doi.org/10.1016/j.neuroimage.2023.120290

Zhu, Y., Wu, D., Sun, K., Chen, X., Wang, Y., He, Y., & Xiao, W. (2023). Alpha and Theta Oscillations Are Causally Linked to Interference Inhibition: Evidence from High-Definition Transcranial Alternating Current Stimulation. *Brain Sciences*,

13(7), Article 7. https://doi.org/10.3390/brainsci13071026

Zivony, A., & Lamy, D. (2022). What processes are disrupted during the attentional blink? An integrative review of event-related potential research. *Psychonomic Bulletin & Review*, *29*(2), 394–414. https://doi.org/10.3758/s13423-021-01973-2

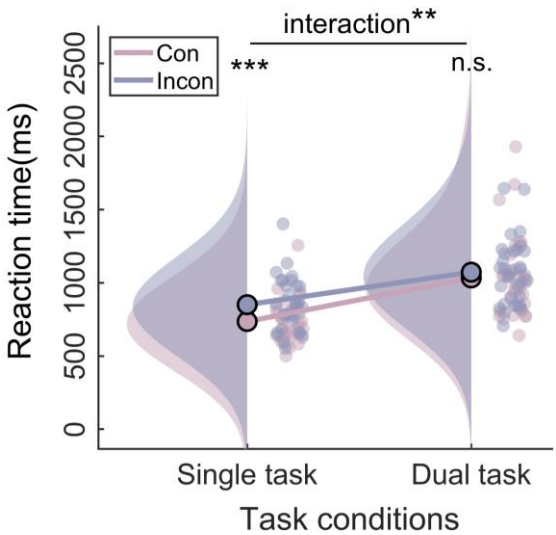

Fig. 1. Raincloud plots (Allen et al., 2021) of behavioral Data. The plot consists of a probability density plot, a line graph, and raw data points. ** $p < 0.01$, *** $p < 0.001$.

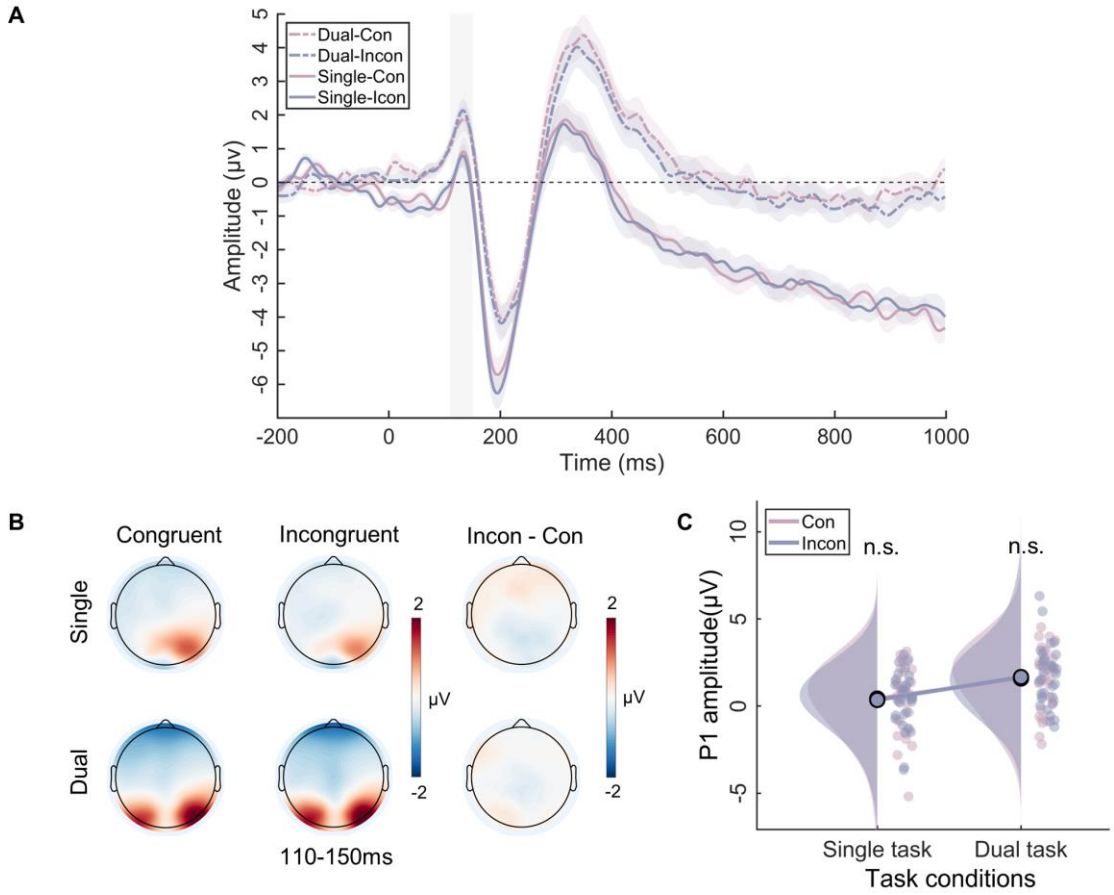

Fig. 2. The P1 results in the single task and the dual task. (A) The event-related potential (ERP) waveforms for P1 component. The shaded rectangle represents the defined time windows and the shading above and below the ERP waveform represents the 95% confidence intervals. (B) Topographic distributions of average amplitude for each condition within the time window (110-150 ms) and the amplitude differences between congruent and incongruent trials in single and dual tasks. (C) Raincloud plots of amplitude for P1 across conditions. n.s., not significant.

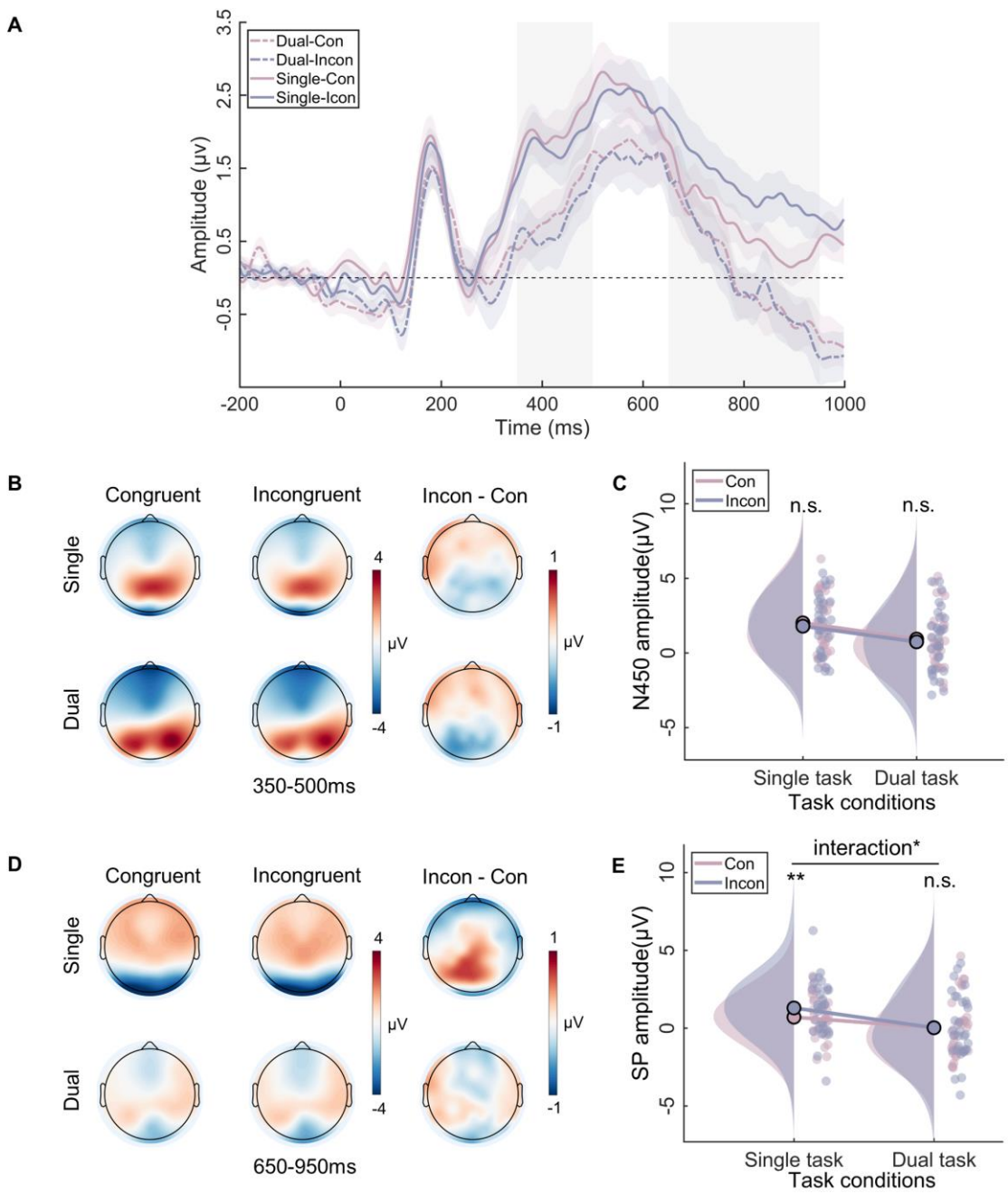

Fig. 3. The N450 and SP results in the single task and the dual task. (A) The event-related potential (ERP) waveforms for P1 and SP components. The shaded rectangle represents the defined time windows and the shading above and below the ERP waveform represents the 95% confidence intervals. (B) Topographic distributions of average amplitude for each condition within the time window (350-500 ms) and the amplitude differences between congruent and incongruent trials in single and dual tasks. (C) Raincloud plots of amplitude for N450 across conditions. (D) Topographic distributions of average amplitude for each condition within the time window (650-950 ms) and the amplitude differences between congruent and incongruent trials in single and dual tasks. (E) Raincloud plots of amplitude for SP across conditions. n.s., not significant, * $p < 0.05$, ** $p < 0.01$.

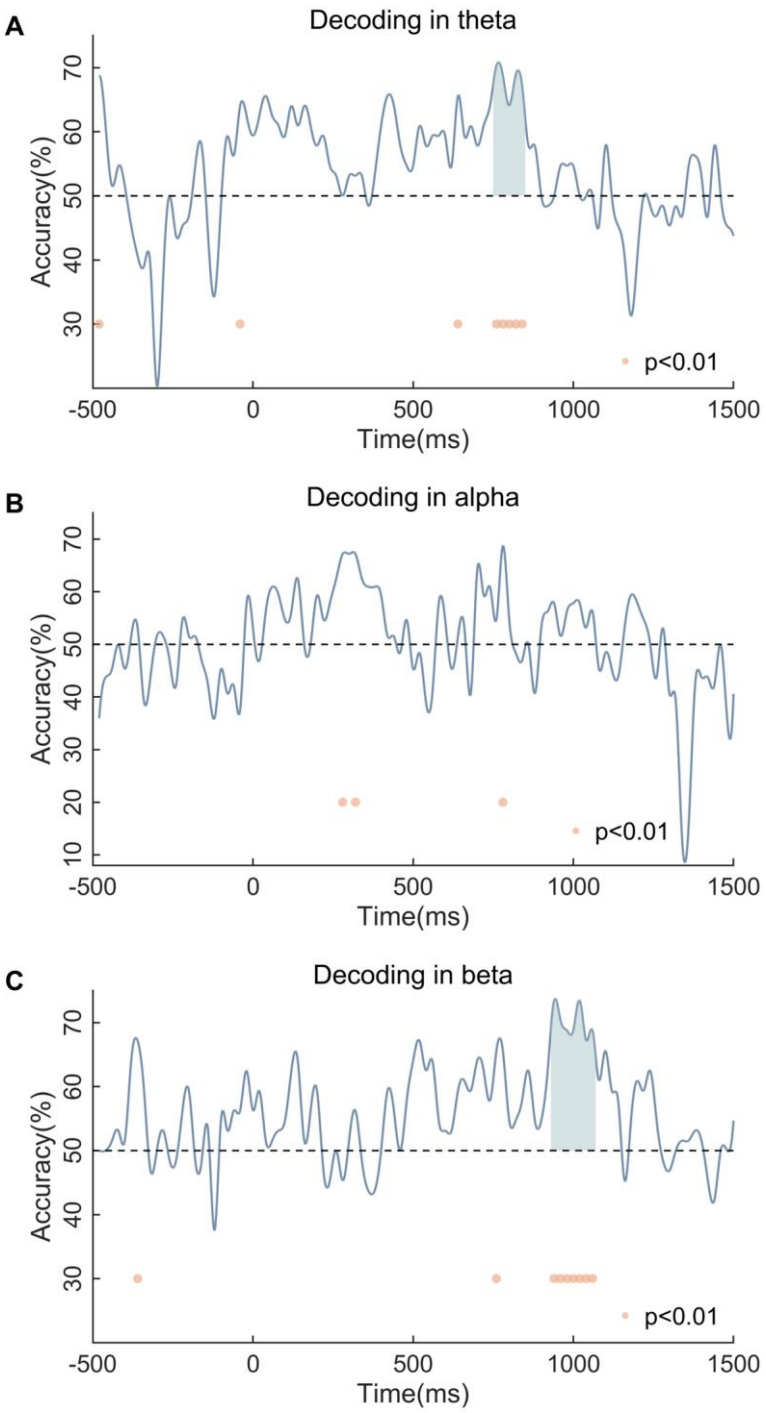

Fig. 4. MVPA results for (A) the theta band, (B) the alpha band, and (C) the beta band. Dots denote significant differences from chance ($P < 0.01$). Shading represents clusters of significant time points (cluster-corrected).

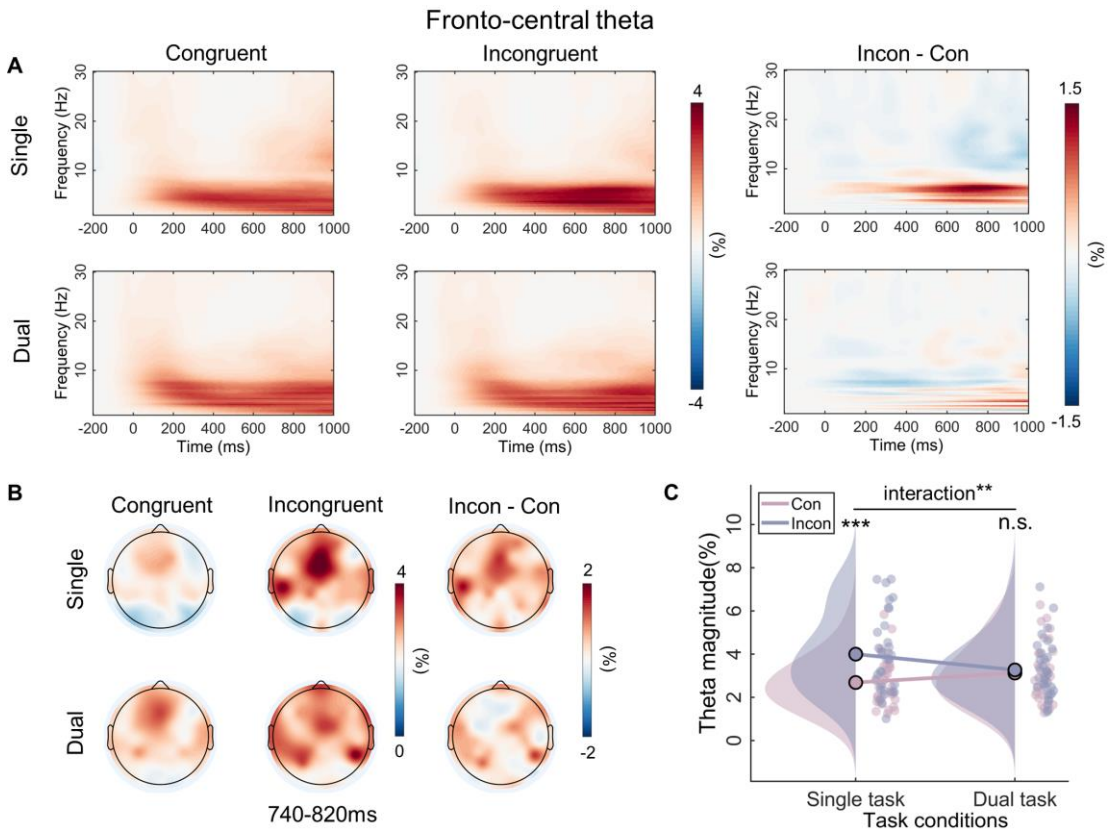

Fig. 5. Time-frequency results for the theta band. (A) Grand-average time-frequency representations for the theta band over fronto-central area (Fz, FCz, Cz) for each condition, and the difference activity between congruent and incongruent trials in single and dual tasks. (B) Topographic distributions of average amplitude for each condition within the defined time-frequency region of interest (4-7 Hz, 740-820 ms) and the magnitude differences between congruent and incongruent trials in single and dual tasks. (C) Raincloud plots of ERSP magnitudes for theta band across conditions. n.s., not significant. ** $p < 0.01$, *** $p < 0.001$.

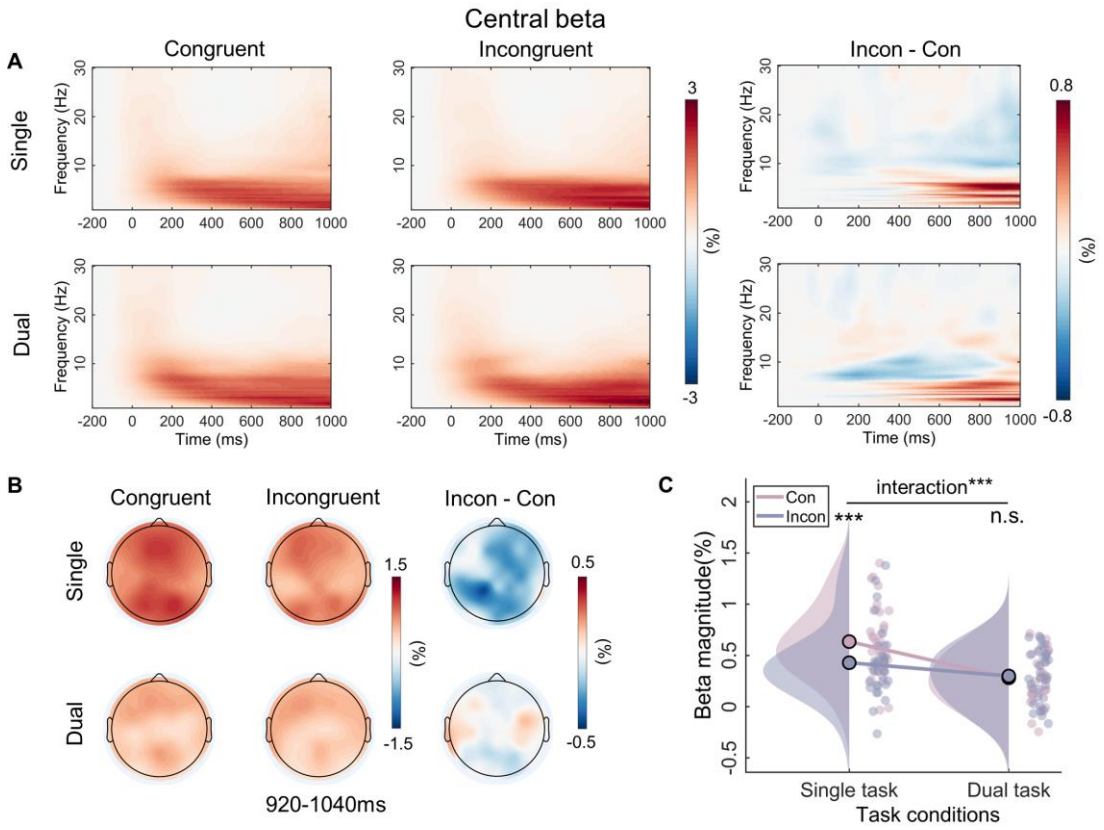

Fig. 6. Time-frequency results for the beta band. (A) Grand-average time-frequency representations for the beta band over the central area (C3, CP3, Cz, CP4, C4) for each condition, and the difference activity between congruent and incongruent trials in single and dual tasks. (B) Topographic distributions of average amplitude for each condition within the defined time-frequency region of interest (14-25 Hz, 920-1040 ms) and the magnitude differences between congruent and incongruent trials in single and dual tasks. (C) Raincloud plots of ERSP magnitudes for the beta band across conditions. n.s., not significant. *** $p < 0.001$.

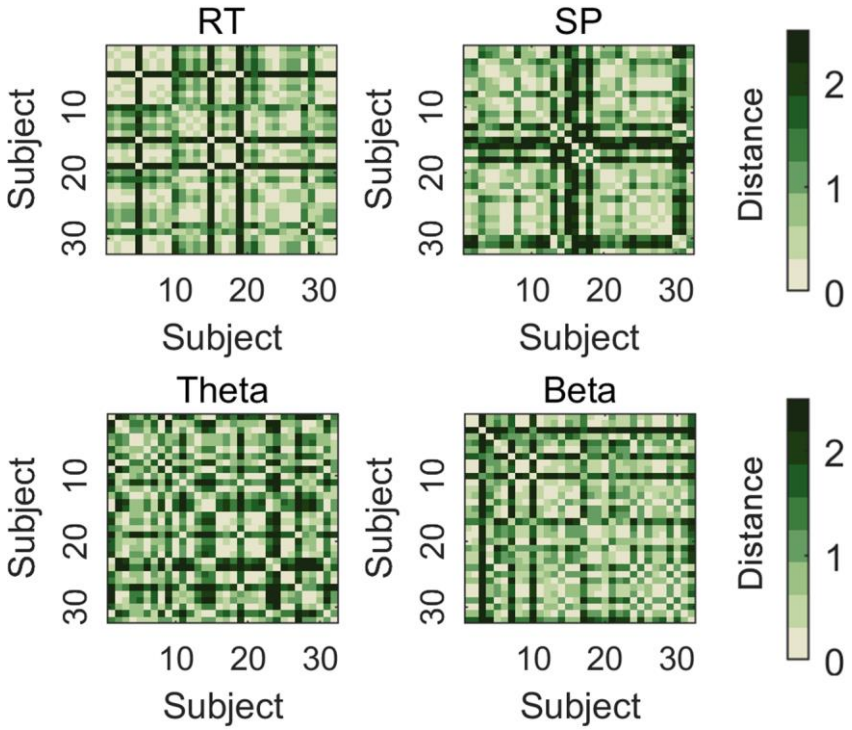

Fig. 7. Representational dissimilarity matrices for the interaction pattern in RT, SP, theta and beta. Each RDM is calculated as the Euclidean distances of data reflecting interaction pattern from 32 subjects.

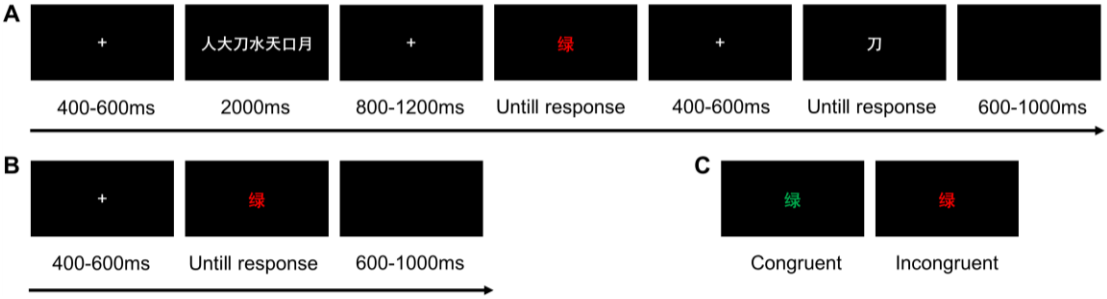

Fig. 8. Schematic illustration of experimental trial structures and stimuli types. (A) Dual-task structure, (B) Single-task structure, (C) Representative stimuli for congruent and incongruent conditions.